

Modelling (001) surfaces of II-VI semiconductors

M. Ahr* M. Biehl T. Volkmann
 Institut für Theoretische Physik und Astrophysik
 Julius-Maximilians-Universität Würzburg
 Am Hubland, 97074 Würzburg, Germany

November 19, 2018

Abstract

First, we present a two-dimensional lattice gas model with anisotropic interactions which explains the experimentally observed transition from a dominant $c(2 \times 2)$ ordering of the CdTe(001) surface to a local (2×1) arrangement of the Cd atoms as an equilibrium phase transition. Its analysis by means of transfer-matrix and Monte Carlo techniques shows that the small energy difference of the competing reconstructions determines to a large extent the nature of the different phases. Then, this lattice gas is extended to a model of a three-dimensional crystal which qualitatively reproduces many of the characteristic features of CdTe which have been observed during sublimation and atomic layer epitaxy.

Within the last years, potential applications of electronic devices based on II-VI semiconductors have inspired basic research concerning for instance the surface reconstructions of these materials. For CdTe, a fairly complete qualitative phase diagram of (001) surfaces has been obtained [1]. An understanding of the interplay of these reconstructions with techniques like molecular beam epitaxy (MBE) or atomic layer epitaxy (ALE) is desirable both for technological applications and for the theory of crystal growth. From the theoretical point of view, the case of CdTe is especially interesting, since it exhibits a phase transition which involves competing reconstructions at typical MBE growth temperatures. While there have been a few models of MBE, especially for GaAs which take into account the effects of surface reconstructions (e.g. [2]), phase transitions between different reconstructions have not been considered in growth

models, so far.

The zinc-blende lattice of CdTe consists of alternating layers of Cd and Te atoms the positions of which lie on regular square lattices. Under vacuum, the CdTe(001) surface is always Cd terminated. The surface is characterized by vacancy structures where the maximum Cd coverage ρ_{Cd} is $1/2$. At low temperature, one finds a $c(2 \times 2)$ reconstruction, where the Cd atoms arrange in a checkerboard pattern. Above a critical temperature $T_c = 543K$ [4] the surface is dominated by a local (2×1) ordering where the Cd atoms arrange in rows along the [110] direction which alternate with rows of vacancies [1, 3, 4]. Electron diffraction experiments have shown that there is a high degree of disorder in the (2×1) phase [4]. This suggests an interpretation of the reordering as an order-disorder phase transition. An external Cd flux stabilizes the $c(2 \times 2)$ reconstruction at $T > T_c$. If a Te flux is applied, one finds surfaces terminated by Te dimers or trimers [1, 3].

*Corresponding author. Phone: +49 (0) 931 888 4908 Fax: +49 (0) 931 888 5141 E-mail: ahr@physik.uni-wuerzburg.de

We first investigate whether the above mentioned transition can be explained within the framework of thermodynamic equilibrium. In a simplifying manner we treat the terminating Cd layer of the surface as a two-dimensional square lattice gas with sites either being occupied by a Cd atom or empty [5]. Chemical bonds and the influence of the underlying crystal are accounted for by effective pairwise anisotropic interactions. An infinite repulsion excludes nearest neighbour (NN) pairs in $[1\bar{1}0]$ -direction (denoted as y -direction in the following). This can be justified from considerations like the electron counting rule [1]. In $[110](x)$ -direction an attractive interaction $\epsilon_x < 0$ favors the occupation of NN sites. A competing attractive interaction $\epsilon_d < 0$ between diagonal neighbors (NNN) tends to stabilize the $c(2 \times 2)$ arrangement. The total energy of the system then reads

$$H = \epsilon_d n_{Cd,d} + \epsilon_x n_{Cd,x} - \mu n_{Cd}, \quad (1)$$

where n_{Cd} , $n_{Cd,d}$ and $n_{Cd,x}$ denote the total number of Cd atoms, NNN and NN pairs in x-direction, respectively. The (effective) chemical potential μ controls the mean Cd coverage $\rho_{Cd} = \langle n_{x,y} \rangle$. By choosing $\epsilon_d = -1$ the energy scale is fixed. In agreement with DFT calculations [6], ϵ_x is chosen such that perfect $c(2 \times 2)$ and (2×1) arrangements are nearly degenerate, the groundstate being a $c(2 \times 2)$ reconstruction.

Besides the coverage ρ_{Cd} the system is characterized by the two-point correlations $C_{Cd}^x = n_{Cd,x}/n_{Cd}$ and $C_{Cd}^d = n_{Cd,d}/n_{Cd}$ which determine the fraction of Cd atoms incorporated in locally (2×1) - or $c(2 \times 2)$ -ordered regions.

Through transfer-matrix (TM) calculations and Monte Carlo (MC) simulations at constant ρ_{Cd} we obtain an estimate of the phase boundaries in the temperature-coverage plane (see fig. 1). At low temperatures (III), a $c(2 \times 2)$ ordered phase with $\rho_{Cd} \approx 1/2$ coexists with a disordered phase of low coverage. At higher temperatures, the system becomes homogeneously disordered (II) or ordered (I) depending on the coverage. For a range of coverages ρ_{Cd} the transition from (III) to (II) is accompanied by a sudden decrease of C_{Cd}^d and a simultaneous increase of C_{Cd}^x , meaning that for these values of ρ_{Cd}

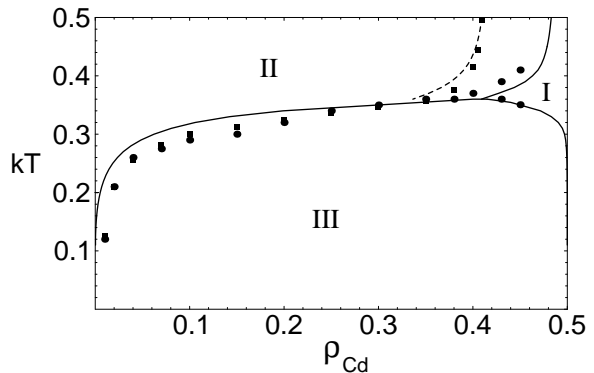


Figure 1: Phase diagram of the 2D lattice gas with $\epsilon_x = -1.90$. Solid lines and circles represent the phase boundaries, obtained from TM and MC. Right of the dashed line (squares) the $c(2 \times 2)$ structure is prevalent and vice versa.

the (2×1) -structure is *locally* prevailing in the disordered regime (the area left of the dashed line (or squares) in fig. 1). With decreasing $|\epsilon_x|$ the tricritical point, i.e. the point in the ρ_{Cd} - T -diagram where (I),(II) and (III) meet, shifts to smaller coverage and higher temperature. Even more so does the line which separates $c(2 \times 2)$ from (2×1) prevalence. This might explain, why a transition from $c(2 \times 2)$ to (2×1) prevalence has not been found in ZnSe, so far. There, the energy difference between perfect $c(2 \times 2)$ and (2×1) reconstructions is indeed greater than for CdTe [6].

In order to investigate the evolution of the morphology of the surface in non-equilibrium processes like growth and sublimation, we extend the planar lattice gas to a model of a three-dimensional crystal. In a previous publication, this has been done for a simple cubic crystal which consists of alternating layers of the two atomic species [8]. In this paper, we present the next step towards a realistic modelling of CdTe by simulating the correct zinc-blende lattice structure. Besides the Cd-Te bond (binding energy ϵ_c) we consider interactions between atoms on NN and NNN sites in one layer of the crystal. The basic idea here is to model the interactions of Cd atoms on the surface with the anisotropic interactions ϵ_x ,

ϵ_d and a hardcore repulsion in the y -direction while there is an isotropic attraction between Te atoms ($\epsilon_{Te,b}$) and Cd atoms inside the bulk of the crystal ($\epsilon_{Cd,b}$).

Due to the topology of the zinc-blende lattice the condition of *ergodicity* can not be fulfilled within the limits of a solid-on-solid (SOS) model, where each atom must be bound to at least two atoms of the opposite species in the layer below. This can be achieved by considering the formation of Te trimers which have been observed experimentally. Additionally, we consider Te atoms which have only one bond to a neighbouring Cd atom. In the following, Te atoms in these configurations will be denoted as Te^* atoms. Te^* atoms neutralize the hardcore repulsion between Cd atoms. Otherwise, the deposition of Te on a Cd terminated surface with a $c(2 \times 2)$ reconstruction would be impossible.

As a simplification, we assume that point defects are not incorporated into the crystal. Then, the bulk can be described in a SOS manner, while the Te^* atoms are considered separately. In summary, the Hamiltonian of the model is

$$H = \epsilon_c n_c + \epsilon_{Cd,b} n_{Cd,b} + \epsilon_{Te,b} + \epsilon_h n_{Cd,h} + \epsilon_x n_{Cd,x} + \epsilon_d n_{Cd,d} + \epsilon^* n^* \quad (2)$$

which is a function of the numbers of Cd-Te bonds (n_c), Te^* atoms (n^*), NN and NNN pairs of surface Cd atoms ($n_{Cd,x}$, $n_{Cd,d}$), NN pairs of Cd atoms in the bulk and Te atoms ($n_{Cd,b}$, $n_{Te,b}$) and surface Cd atoms next to incorporated Cd atoms ($n_{Cd,h}$). Pairs of surface Cd atoms which are not bound to Te^* atoms on neighbour sites in the y -direction are forbidden.

Besides the deposition of adatoms we consider desorption, diffusion to NN and NNN sites and diffusion across steps. These are Arrhenius-activated processes with rates $\nu \exp[-E/(kT)]$. Desorption requires an activation energy $E = \Delta H$. We have chosen Metropolis-like energy barriers $E = \max\{B, B + \Delta H\}$ for diffusion processes. There is a barrier $B = B_0$ for the diffusion of atoms with two bonds and a barrier B^* for the diffusion of Te^* atoms.

Unfortunately, the available experimental data are not sufficient for a systematic fit of the model pa-

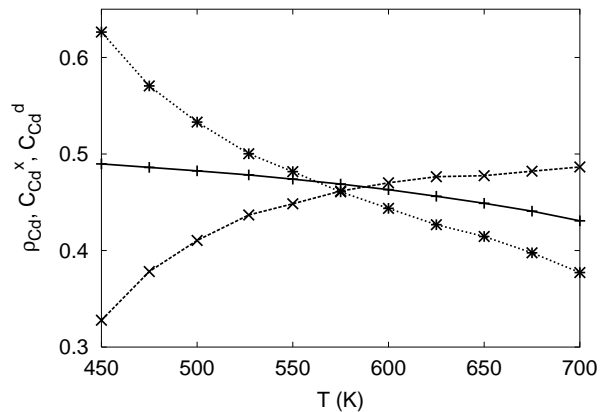


Figure 2: ρ_{Cd} (+) and the correlations C_{Cd}^x (x), C_{Cd}^d (*) as functions of temperature in the stationary state of sublimation. The system size was 64×64 .

rameters and there are no values of diffusion barriers available from ab initio or semi-empirical calculations. Therefore, the choice of the parameter set is partly based on estimates and physical reasoning. In the following, we present results that have been obtained with the parameter set $\epsilon_d = -0.086eV$, $\epsilon_x = -0.168eV$, $\epsilon_{Cd,b} = \epsilon_{Te,b} = -0.069eV$, $\epsilon_h = 0$, $\epsilon_c = -0.43eV$, $\epsilon^* = -0.26eV$, $B_0 = 0.78eV$, $B^* = 0.17eV$ and $\nu = 10^{12}/s$.

Experiments have revealed a high density of steps on CdTe surfaces with a preferential orientation in the (100) direction. This leads to a dominant contribution of step flow sublimation. Therefore, we have simulated sublimation on vicinal surfaces with steps parallel to the [100] direction at a distance of 16 lattice constants.

Our model reproduces the observation of Cd terminated surfaces in vacuum. A Te terminated surface decays in a temperature-dependent time interval $\tau(T)$. The corresponding desorption probability $p(T) \sim 1/\tau(T)$ follows an Arrhenius law with an activation energy of $1.25 \pm 0.02eV$. After this onset, we obtain a stationary state where Cd and Te evaporate stoichiometrically. Then, the temperature dependence of the sublimation rate follows an Arrhenius law with a higher activation energy of $1.437 \pm 0.003eV$. Experimentally, activation energies

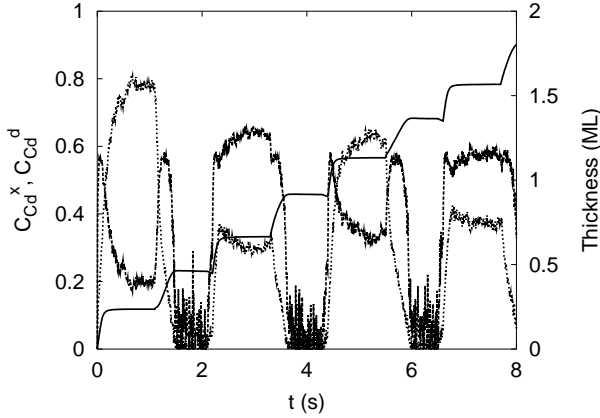


Figure 3: Correlations C_{Cd}^x (dashed), C_{Cd}^d (dotted) and thickness of the deposited layer (solid) in ALE as a function of time. The pulse time was 1s, followed by 0.1s of dead time, the system size was 128×128 .

of $1.54eV$ [4] and $0.9eV$ [3] have been found for stoichiometric step flow sublimation and the decay of a Te terminated surface.

Figure 2 shows ρ_{Cd} and the correlations C_{Cd}^x , C_{Cd}^d in the stationary state as functions of T . In the investigated temperature interval, ρ_{Cd} decreases only slightly from $\rho_{Cd} = 0.49$ at $T = 450K$ to $\rho_{Cd} = 0.43$ at $T = 700K$. At low temperature, the surface is dominated by a $c(2 \times 2)$ arrangement of the Cd atoms ($C_{Cd}^d > C_{Cd}^x$). On the contrary, at high temperature the Cd atoms tend to arrange in the rows of the (2×1) reconstruction ($C_{Cd}^d < C_{Cd}^x$). The crossover between both regimes is at $T_c = 570K$. This is the counterpart of the phase transition observed in the 2D lattice gas model. However, an investigation of C_{Cd}^x , C_{Cd}^d in the 2D lattice gas at the ρ_{Cd} measured in the 3D model shows, that the non-equilibrium conditions of sublimation increase the dominance of (2×1) over $c(2 \times 2)$ in the high temperature regime.

ALE provides a scenario where our model can be investigated in a situation present in technical applications. The basic idea is to obtain self-regulated layer-by-layer growth by alternate deposition of pure Cd and Te. Figure 3 shows the evolution of the thickness of the deposited layer and the correlations C_{Cd}^x , C_{Cd}^d at $T = 500K < T_c$. The initial state was a flat

Te terminated surface. In the first phase, a Cd flux of $5ML/s$ is applied, in the second phase Te at the same rate. At the end of the first phase, the surface is Cd terminated with a $c(2 \times 2)$ reconstruction. In the Te phase, Te terminated islands form which, at the end of the cycle, cover $\approx 50\%$ of the surface. This is due to the fact that only half of the Cd atoms needed for a closed monolayer are present. Note, that the decrease of ρ_{Cd} at the beginning of the Te cycle leads to an increase of C_{Cd}^x , which is consistent with the phase diagram (fig. 1) of the 2D lattice gas. In the following Cd phase, the islands are covered with Cd. Surprisingly, now the reconstruction is (2×1) . This can be understood from the fact that the lattice gas interactions are present only between particles in the same layer. Thus, the island edges impose open boundary conditions to the lattice gas of Cd atoms on the island. In contrast to a $c(2 \times 2)$ reconstructed domain, a (2×1) terminated island can reduce the energy of its boundary by elongating in x -direction. Since the ground state energies of both structures are nearly degenerate, the formation of (2×1) may thus reduce the surface free energy. In the following Te phase, Cd and Te atoms diffuse into the gaps between the islands, which leads to the formation of a closed, Te covered monolayer again. These observations closely resemble ideas suggested in [9] to explain experimental observations.

In summary, we have presented a model of CdTe(001) surfaces which reproduces several experimental observations in a semi-quantitative way. In the future, we will extend this model by considering the dimerization of surface Te atoms and the fact that Te is adsorbed and desorbed as Te_2 . In cooperation with an experimental group, we will try a more quantitative determination of an appropriate parameter set.

References

- [1] J. Cibert, S. Tatarenko. Defect and Diffusion Forum **150-151**, 1, 1997 and references therein.
- [2] P. Kratzer, E. Penev, M. Scheffler. preprint, cond-mat/0105430

- [3] S. Tatarenko, B. Daudin, D. Brun, V. Etgens, M. B. Veron. Phys. Rev. B **50**, 18479, 1994
- [4] H. Neureiter, S. Tatarenko, S. Spranger, M. Sokolowski. Phys. Ref. B **62**, 1542, 2000
- [5] M. Biehl, M. Ahr, W. Kinzel, M. Sokolowski. T. Volkmann, Europhys. Lett. **53**(2), 169, 2001
- [6] S. Gundel, A. Fleszar, W. Faschinger, W. Hanke. Phys. Rev. B **59**, 15261, 1999
- [7] N. C. Bartelt, T. L. Einstein, L. D. Roelofs. Phys. Rev. B **34**, 1616, 1986
- [8] M. Ahr, M. Biehl. Surf. Sci. **488**, L553, 2001
- [9] M. B. Veron, A. Arnoult, B. Daudin, S. Tatarenko. Phys. Rev. B **54**(8), R5267, 1996